nature immunology

Conditioning of naive CD4+ T cells for enhanced peripheral Foxp3 induction by nonspecific bystander inflammation

Lucas J Thompson[1,4], Jen-Feng Lai[1,4], Andrea C Valladao[1,2], Tennille D Thelen[1,2], Zoe L Urry[3] & Steven F Ziegler[1]

Inflammation induced during infection can both promote and suppress immunity. This contradiction suggests that inflammatory cytokines affect the immune system in a context-dependent manner. Here we show that nonspecific bystander inflammation conditions naive CD4+ T cells for enhanced peripheral Foxp3 induction and reduced effector differentiation. This results in inhibition of immune responses *in vivo* via a Foxp3-dependent effect on antigen-specific naive CD4+ T cell precursors. Such conditioning may have evolved to allow immunity to infection while limiting subsequent autoimmunity caused by release of self-antigens in the wake of infection. Furthermore, this phenomenon suggests a mechanistic explanation for the idea that early tuning of the immune system by infection affects the long-term quality of immune regulation.

The adaptive immune system has evolved to provide effective long-term resistance to a wide range of microbial infections. However, the vigor of the immune response must be balanced by mechanisms that prevent damage to self-tissues. These mechanisms include intrinsic negative feedback pathways that 'shut down' inflammatory signals[1,2], as well as mobilization of regulatory Foxp3+ T cells (T_{reg} cells) that can suppress effector T cell (T_{eff} cell) responses[3]. The peripheral differentiation of naive CD4+ T cells into Foxp3+ T_{reg} cells serves to enhance the functional capacity of the total T_{reg} cellular pool by broadening the clonal repertoire[4]. This process critically limits immunopathology in tissues and at mucosal sites by induction of antigen-specific T_{reg} cells that enforce tolerance to self-antigens or innocuous foreign antigens[5]. Peripheral development of T_{reg} cells has an important role in immune tolerance overall, but it is unclear how antigen-specific T_{reg} cells from naive CD4+ T cell precursors are modulated during the course of an acute inflammatory response such as to viral infection.

Viral infection and immunostimulatory agents such as Toll-like receptor (TLR) agonists promote T cell responses in part by production of cytokines[6]. Inflammatory cytokines and type I interferon (IFN-I) released by TLR stimulation enhance T_{eff} cell responses and counteract development and function of T_{reg} cells that express the transcription factor Foxp3 (refs. 7–9). TLR agonists such as the 'viral mimic' polyinosinic:polycytidylic acid (poly(I:C)) generate IFN-I inflammation and are promising candidates to augment vaccination[10]. However, inflammatory cytokines also generate bystander signals to naive T cells not specific for viral antigens[11]. This may act to breach activation thresholds for self-reactive T cells, supporting the notion that infection can trigger autoimmunity[12,13]. In contrast, antiviral inflammatory responses have also been shown to cause immunosuppression[12,14]. This contradiction suggests that inflammatory cytokines may affect T cell responses in a flexible manner, with the outcome dependent on the context of T cell response.

Here we show that nonspecific bystander inflammation conditions naive CD4+ T cells for diminished effector response and enhanced induction of Foxp3 in response to subsequent antigen encounter. We refer to these T cells as inflammation-conditioned naive T ($_{IC}T_N$) cells. The phenotypic change is directed by antiviral inflammatory signals and depends on IFN-I signaling. Naive CD4+ T cells exposed to IFN-I bystander inflammation showed changes in molecular pathways that diminished T_{eff} cell development to 'favor' *de novo* T_{reg} cell development from naive CD4+ T cell precursors, thereby affecting subsequent antigen-specific immune responses. These data suggest that naive CD4+ T cells integrate signals over time during an immune response to modulate effector and regulatory cellular responses over the course of inflammation.

RESULTS

Effects of inflammation on Foxp3+ T_{reg} cells and asthma

To determine the role of nonspecific inflammatory stimuli on CD4+ T cells, we induced systemic inflammation in mice by intraperitoneal injection of poly(I:C). After this treatment, we observed a notable increase in frequency and total numbers of functional Foxp3+CD4+ T cells in the spleen, peaking ~7 d after injection (**Supplementary Fig. 1a**). Foxp3+ T_{reg} cells sorted from mice treated with poly(I:C) showed similar *in vitro* functional suppressive activity and *ex vivo* phenotype to that of control cells from PBS-treated mice (**Supplementary Fig. 1b–d** and data not shown) and did not produce inflammatory cytokines upon *ex vivo* restimulation (**Supplementary Fig. 1e**).

[1]Benaroya Research Institute, Immunology Research Program, Seattle, Washington, USA. [2]Department of Immunology, University of Washington, Seattle, Washington, USA. [3]Kings College London, London, UK. [4]These authors contributed equally to this work. Correspondence should be addressed to S.F.Z. (sziegler@benaroyaresearch.org).

Received 20 June 2015; accepted 21 October 2015; published online 11 January 2016; doi:10.1038/ni.3329

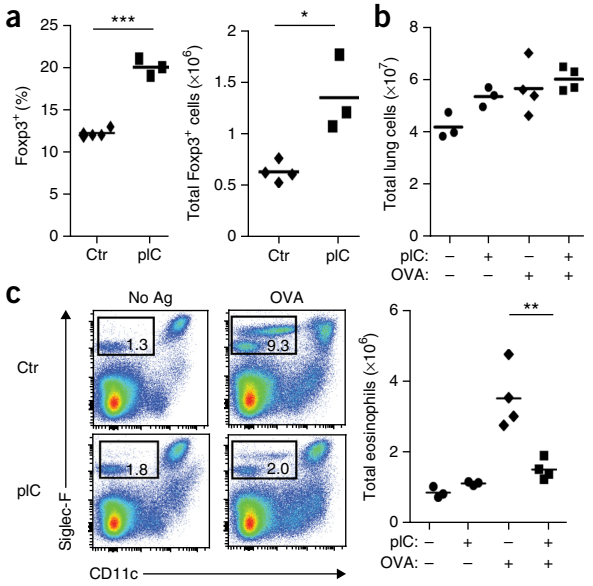

Figure 1 Nonspecific bystander inflammation results in increased Foxp3$^+$ T_{reg} cells and suppression of primary antigen-specific mucosal inflammatory response. (**a**) Frequency (left) and total number (right) of Foxp3$^+$CD4$^+$ T cells from wild-type (WT) BALB/c mice 7 d after treatment with poly(I:C) (pIC) or PBS (ctr) intranasally for two consecutive days. Each symbol represents an individual mouse; data are representative of two independent experiments. (**b**,**c**) Primary antigen-specific pulmonary inflammation after intranasal pIC (+) or PBS (–) and challenge with OVA–TSLP (+) or PBS (–) (Online Methods and **Supplementary Fig. 1f**), as indicated by total pulmonary cell counts for mononuclear cells (**b**) and flow cytometry analysis of pulmonary eosinophil infiltration (**c**, left) and total eosinophil count (**c**, right; OVA, OVA rechallenge; no Ag, no antigen rechallenge). Outlines and numbers on flow cytometry plots indicate percentage of eosinophils in gated region. Each symbol represents an individual mouse, horizontal bars represent group mean; data are representative of two independent experiments, $n \geq 6$ mice per group. $^*P < 0.05$, $^{**}P < 0.01$, $^{***}P < 0.001$, Student's two-tailed *t*-test.

When poly(I:C) was delivered directly (intranasally) to the pulmonary mucosa, we observed increased frequencies and numbers of Foxp3$^+$ T_{reg} cells in the lungs of mice (**Fig. 1a**). To determine how this nonspecific bystander inflammatory effect affected a primary immune response in the mucosal environment, we adapted a model of antigen-specific priming via pulmonary mucosa after intranasal poly(I:C) treatment[15] (Online Methods and **Supplementary Fig. 1f**). All treatments resulted in a trend of elevated pulmonary cellular infiltration in poly(I:C)-treated mice as compared to PBS-treated negative controls (**Fig. 1b**). Primary antigen delivery resulted in eosinophil accumulation as well as other measures of pulmonary inflammation in positive control (PBS pretreated) mice, and this response was completely inhibited in mice pretreated with poly(I:C) (**Fig. 1c**). This effect was not due to skewing of lung infiltration toward a neutrophilic-based response (**Supplementary Fig. 1g**), which indicates that bystander inflammation shut down, rather than qualitatively altered, the airway inflammatory response[16].

Immunization after inflammation diminishes recall response

We next tested the impact of systemic bystander inflammation on antigen-specific recall immune responses. Mice were treated with PBS or poly(I:C) via intraperitoneal injection, followed by immunization with subcutaneous ovalbumin (OVA) emulsified in incomplete Freund's adjuvant (IFA). The mice were challenged with antigen 7–10 d later either via the airways or implanted with antigen-expressing tumor, and airway inflammation or tumor growth were assessed (Online Methods and **Supplementary Fig. 2a**). Upon intranasal antigen challenge, mice that were primed with antigen after bystander inflammation showed lower total pulmonary cellularity (**Fig. 2a**) and eosinophil (**Fig. 2b**) and neutrophil (**Fig. 2c**) infiltration than controls, which indicates that the immune-suppressive effect of poly(I:C)-mediated inflammation can inhibit antigen-specific mucosal recall responses that are anatomically disparate. Similarly, poly(I:C)-treated mice showed a modest but significant decrease in tumor resistance after challenge with OVA-expressing A20 lymphoma[17], compared to controls (**Fig. 2d** and **Supplementary Fig. 2b**). These observations show that qualitatively diverse endogenous antigen-specific immune responses are suppressed *in vivo* when priming occurs after nonspecific bystander inflammation.

Inflammation alters molecular pathways in naive CD4$^+$ T cells

The marked impact of nonspecific inflammation on antigen-specific responses and increase in Foxp3$^+$ T_{reg} cells, at mucosal sites in particular, suggested a potential impact of bystander inflammation on the priming of naive T cells. To determine how nonspecific bystander inflammation affects naive CD4$^+$ T cells, we treated recombination-activated gene-deficient DO11.10 T cell–antigen receptor (TCR)-transgenic (DR) mice with poly(I:C) and used them as a source of naive non-T_{reg} CD4$^+$ T cells stimulated with bystander inflammation in the absence of cognate antigen (i.e., $_{IC}T_N$ cells) (**Supplementary Fig. 3a**).

We first investigated the *ex vivo* expression of genes associated with regulation of T cell activation. Negative signal feedback molecules, such as Socs1 (encoded by *Socs1*) and microRNA 155 (*MiR155*), modulate effector T cell responses and support T_{reg} cell stability and function[18,19]. Expression of *Socs1* and *Mir155* was higher in directly isolated *ex vivo* $_{IC}T_N$ DR CD4$^+$ T cells than in controls from PBS-treated mice (**Fig. 3a**,**b**). Next, we examined mTOR signaling in antigen-stimulated CD4$^+$ T cells by assessment of phosphorylated S6 riboprotein (p-S6) and p-AKT. Suppression of AKT-mTOR activation downstream of antigen

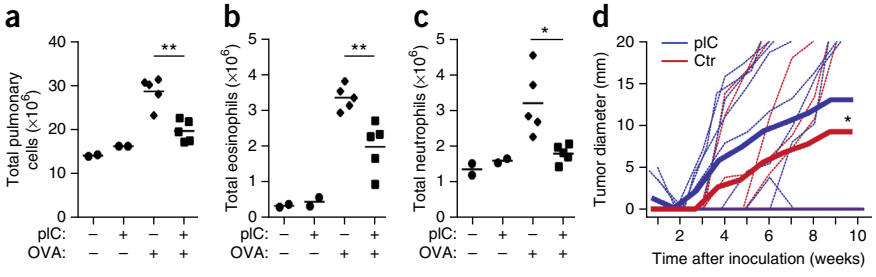

Figure 2 Immunization after nonspecific bystander inflammation results in diminished antigen-specific recall response (**Supplementary Fig. 2a**). (**a**–**c**) Airway response of mice challenged with intranasal OVA after OVA immunization in the context of PBS or poly(I:C) (pIC) pretreatment, as indicated by total pulmonary cell counts for mononuclear cells (**a**), eosinophils (**b**) or neutrophils (**c**). Each symbol represents a single mouse. Data are representative of two independent experiments, $n \geq 4$ mice per group. (**d**) Growth of OVA-bearing A20-tGO tumor after OVA immunization in the context of PBS or pIC pretreatment. Dotted lines represent individual mice, thick lines represent mean tumor size for all mice. Data are compiled from two independent experiments, $n = 11$ mice per group. $^*P < 0.05$, $^{**}P < 0.001$, Student's two-tailed *t*-test (**a**–**c**) or two-way ANOVA (**d**).

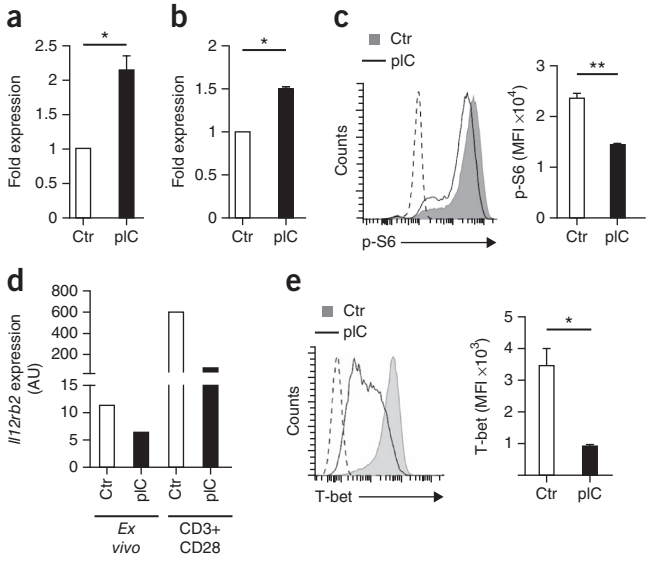

Figure 3 $_{IC}T_N$ show altered molecular pathways that instruct T cell differentiation. (**a**,**b**) Expression of *Socs1* mRNA (**a**) and *Mir155* (**b**) in naive CD4$^+$ T cells isolated from DR mice treated with PBS (ctr) or poly(I:C) (pIC) (**Supplementary Fig. 3a**). Expression is shown relative to corresponding control DR cells (set to 1) and normalized to *Rn18s* (**a**) or *Sno234* RNA (**b**). (**c**) Flow cytometry analysis of intracellular p-S6 (left) and mean florescence intensity (MFI) of p-S6 staining (right) in DR cells stimulated with OVA(323-339) peptide-pulsed APCs for 16 h. (**d**) *Il12rb2* expression in $_{IC}T_N$ mice, normalized to *Rn18s* RNA. RNA was extracted from purified DR cells directly *ex vivo* or after 48 h of stimulation with plate-bound anti-CD3 and CD28 (CD3+CD28) *in vitro*. Data are representative of three independent experiments. AU, arbitrary units. (**e**) Flow cytometry analysis (left) and MFI of T-bet staining (right) in DR cells stained for intracellular T-bet after 3 d of OVA peptide stimulation. Dashed line indicates unstimulated control cells (**c**,**e**). Data are representative of at least three independent experiments, $n \geq 3$ mice per group (**a**–**e**); error bars, mean and s.e.m. of three replicates. $^*P < 0.01$, $^{**}P < 0.001$, Student's two-tailed *t*-test.

receptor signaling pathways results in enhanced Foxp3$^+$ T_{reg} cell (as opposed to T_{eff} cell) differentiation[20,21]. Upon antigen stimulation, p-S6 was reduced in $_{IC}T_N$ DR cells (**Fig. 3c**). We also observed a modest but consistent reduction in AKT activation (**Supplementary Fig. 3b**). Additionally, after antigen stimulation, expression of *Il12rb2* mRNA and T-bet protein[22,23], which enable effector T_H1 differentiation and repress T_{reg} cell differentiation, was substantially reduced in $_{IC}T_N$ DR cells (**Fig. 3d**,**e**). These changes in cellular responsiveness occurred despite similar rates of proliferation and cell survival (**Supplementary Fig. 3c**,**d**). Together, these data suggest that nonspecific bystander inflammation conditions naive T cells into a refractory molecular 'state' that could dampen T cell activation.

$_{IC}T_N$ cells 'favor' T_{reg} cell differentiation

The impact of bystander inflammation on molecular pathways after CD4$^+$ T cell stimulation suggested that the *de novo* differentiation of T_{eff} and T_{reg} cells may be affected in response to antigen. After TCR stimulation in the presence of transforming growth factor-β (TGF-β), $_{IC}T_N$ DR cells showed ~5-fold higher frequency of Foxp3$^+$ cells than did control cells from PBS-treated mice (**Fig. 4a**). This increase did not require the continued presence of antigen-presenting cells (APCs) (**Supplementary Fig. 4a**), which indicates that bystander inflammation imposed a cell-intrinsic physiological state on the naive T cells that resulted in enhanced *de novo* T_{reg} cell generation after encounter with antigen. We also observed this effect with isolated naive CD4$^+$ T cells from poly(I:C)-treated wild-type BALB/c mice (**Fig. 4b**), which indicates that this effect was not an artifact of a transgenic TCR. Notably, these effects were most prominent at suboptimal TGF-β concentrations for T_{reg} cell differentiation. *Foxp3* promoter methylation was similar among naive CD4$^+$ T cells from $_{IC}T_N$ and control DR mice, as well as BALB/c mice, which indicates that this represented conversion of a 'true' naive CD4$^+$ T cell population (**Supplementary Fig. 4b**). These data further suggest that the bystander inflammatory signals do not 'prepare' the *Foxp3* locus for responsiveness by altering DNA methylation.

In agreement with the patterns of molecular activation described above, $_{IC}T_N$ DR cells produced less IFN-γ than control cells when cultured in nonskewing conditions (**Fig. 4c**). When we supplemented culture with TGF-β, we observed low IL-17A production, and this was increased upon addition of IL-6 (ref. 24). In both cases, $_{IC}T_N$ DR cells produced significantly less IL-17A cytokine, even when Foxp3 expression was nearly abolished by addition of IL-6 (**Fig. 4d**). We did not observe changes in expression of the TGF-β receptor *ex vivo* or activation of the signal transducers SMAD2 or SMAD3 with addition of exogenous TGF-β (**Supplementary Fig. 4c**,**d**), which suggests that molecular coordination amplifies the effect of existing TGF-β signaling components in $_{IC}T_N$ cells. Together, these data show that naive CD4$^+$ T cells exposed to bystander inflammation before antigen encounter exhibit enhanced *de novo* T_{reg} cell differentiation.

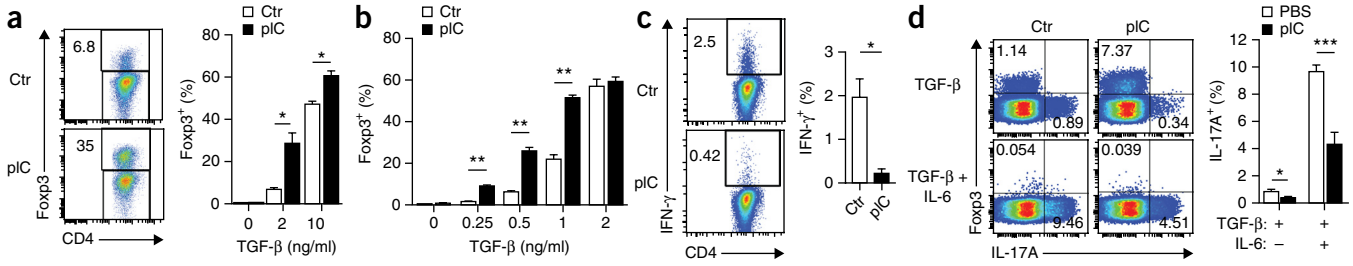

Figure 4 Naive CD4$^+$ T cells exposed to bystander inflammation are conditioned for enhanced *de novo* Foxp3$^+$ T_{reg} cell differentiation and reduced effector helper T cell differentiation. (**a**) Flow cytometry analysis of Foxp3 expression (left) and frequencies (right) of Foxp3$^+$ cells from spleen and lymph node CD4$^+$ T cells from control (ctr) or poly(I:C)-treated (pIC) DR mice stimulated for 5 d with APCs pulsed with OVA peptide and TGF-β. (**b**) Frequency of Foxp3$^+$ cells in naive CD4$^+$ T cells from ctr or pIC-treated BALB/c mice after sorting and culture with plate-bound anti-CD3+CD28 and TGF-β. (**c**) Flow cytometry analysis (left) and quantification (right) of intracellular IFN-γ$^+$ DR cells cultured in nonskewing conditions and stimulated with PMA + ionomycin (P/I). (**d**) Flow cytometry analysis (left) and quantification (right) of intracellular Foxp3 and IL-17A expression in DR cells cultured in the presence of TGF-β or TGF-β + IL-6 then stimulated with P/I. Frequencies of gated populations are indicated by numbers in or adjacent to gates on flow cytometry plots (**a**,**c**,**d**). Data are mean and s.e.m. for three replicates or representative of 3–5 independent experiments, $n \geq 3$ mice per group. $^*P < 0.05$, $^{**}P < 0.001$, $^{***}P < 0.0001$, Student's two-tailed *t*-test.

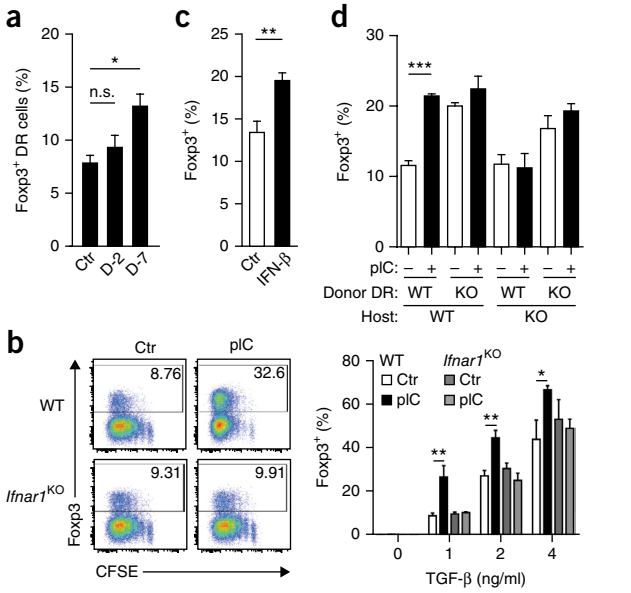

Figure 5 Antiviral bystander inflammation and type I interferon conditions naive T cells for enhanced *de novo* T_{reg} cell differentiation. (**a**) Percentage of Foxp3$^+$ cells among cultured donor DR cells. DR cells were parked in BALB/c host mice, which were then inoculated with LCMV 7 d (D-7) or 2 d (D-2) before harvest; control mice (ctr) were left untreated. CD4$^+$ T cells were isolated and cultured with OVA-pulsed APC and TGF-β for 5 d. (**b**) Flow cytometry analysis (left) and quantification of (right) Foxp3$^+$ DR cells in CD4$^+$ T cells from ctr and poly(I:C)-treated (pIC) wild-type (WT) and *Ifnar1*^{KO} mice (**Supplementary Fig. 3a**) stained for Foxp3 after 5 d. Frequencies of gated populations are indicated by numbers in gates on flow cytometry plots. (**c**) Frequency of Foxp3$^+$ cells in CD4$^+$ T cells after 3-d incubation with OVA-pulsed APC and TGF-β. CD4$^+$ T cells were isolated from DR splenocytes incubated for 48 h with PBS (ctr) or IFN-β. (**d**) Intracellular Foxp3 expression in lymphocytes from WT or *Ifnar1*^{KO} BALB/c host recipients of WT or *Ifnar1*^{KO} DR cells, treated with PBS (ctr) or pIC. Lymphocytes were cultured with OVA-pulsed APCs and TGF-β for 5 d before assessment. Data are mean and s.e.m. of three replicates representative of two independent experiments, $n \geq 2$ mice per group. n.s., not significant; $^*P < 0.05$, $^{**}P < 0.01$, $^{***}P < 0.001$, Student's two-tailed *t*-test.

$_{IC}T_N$ T_{reg} cell differentiation follows viral infection and IFN-I

Poly(I:C) is commonly used as an adjuvant that mimics the effects of viral infection. To address whether enhanced T_{reg} cell induction occurs in a setting of bystander activation during a viral infection, we transferred DR cells into BALB/c hosts, which we then infected with lymphocytic choriomeningitis virus (LCMV). At various times after infection we then isolated CD4$^+$ T cells from these mice and cultured them with OVA peptide–pulsed APCs and TGF-β, similarly to the approach we used with poly(I:C) above. Induced T_{reg} cell differentiation was significantly increased in DR cells from mice infected for 7 d, as compared to earlier and later time points (**Fig. 5a** and data not shown). Although the timing of this effect differed between poly(I:C) treatment and LCMV infection, it is notable that the kinetics of innate inflammatory cytokine expression are such that enhanced T_{reg} cell differentiation occurred soon after the peak of the *in vivo* inflammatory responses of each of these treatments[25,26]. Notably, whereas poly(I:C) and the TLR7 ligand gardiquimod conditioned native T cells for enhanced T_{reg} cell induction, lipopolysaccharide (LPS) did not mediate this effect, which suggests a role for the qualitative nature of the inflammatory milieu in this response (**Supplementary Fig. 5a**).

Poly(I:C) and LCMV specifically activate a substantial IFN-I response[27]. Consistent with a role for IFN-I, incubation of splenocytes with poly(I:C) resulted in enhanced *de novo* T_{reg} cell induction that was blocked by neutralizing antibody against the receptor IFNAR1 (**Supplementary Fig. 5b**). Next, we assessed T_{reg} cell induction in IFNAR1-deficient (*Ifnar1*^{KO}) DR mice treated with poly(I:C). In contrast to wild-type DR cells, *Ifnar1*^{KO} DR cells did not show enhanced T_{reg} cell induction or diminished T_{eff} cell differentiation after poly(I:C) treatment (**Fig. 5b** and **Supplementary Fig. 5c**), which demonstrates a clear dependence on IFN-I signals for this response. $_{IC}T_N$ DR cells showed high expression of *Socs1*, which indicates that expression of these feedback molecules is a consequence of IFNAR1 signaling. Consistent with the consequent upregulation of these negative feedback molecules, and despite similar *Ifnar1* and *Ifnar2* expression, $_{IC}T_N$ DR cells showed lower STAT1 activation after exposure to IFN-β (**Supplementary Fig. 5d,e**). When naive DR spleen cells were cultured *in vitro* with IFN-β, subsequent *de novo* T_{reg} cell induction was enhanced (**Fig. 5c**), which indicates that IFN-I alone is sufficient to elicit this response. A number of anti-inflammatory pathways are induced in response to IFN-I signals, including IL-10, PD-L1 and indolamine-2,3-dioxygenase (IDO). Neutralization of IL-10 or PD-L1 by treatment with blocking antibodies did not abrogate the enhanced Foxp3 induction in $_{IC}T_N$ cells (**Supplementary Fig. 5f**), nor did treatment with IDO inhibitor 1-methyltryptophan (1-MT) (**Supplementary Fig. 5g**). Furthermore, although we observed expression of PD-L1 on $_{IC}T_N$ cells, we were unable to detect expression of *Foxa1* mRNA, which has been described as a mediator of IFN-I–regulated tolerance[28] (data not shown).

To determine whether IFN-I has a direct role on naive CD4$^+$ T cells to condition for enhanced T_{reg} cell induction, we transferred wild-type or *Ifnar1*^{KO} DR CD4$^+$ T cells into wild-type or *Ifnar1*^{KO} BALB/c host mice. These mice were treated with poly(I:C), and T cells were cultured with OVA-pulsed APCs and TGF-β. Using Ly6C as a surrogate marker for bystander inflammation among the donor DR cells[29], we observed that wild-type DR cells were responsive to bystander inflammatory signals in both wild-type and *Ifnar1*^{KO} host environments, whereas *Ifnar1*^{KO} DR cells showed only mild activation in the wild-type hosts and no activation in *Ifnar1*^{KO} hosts (**Supplementary Fig. 5h**). Despite the apparent acquisition of some IFN-I–mediated bystander activating signals, we observed enhanced T_{reg} cell induction only among wild-type DR cells in the wild-type host environment for $_{IC}T_N$ cells versus controls (**Fig. 5d**), which suggests a role for IFN-I signaling in multiple cell types for coordination of this effect. In contrast, direct IFN-I signals seemed to be involved in the conditioning of naive CD4$^+$ T cells for diminished effector activity (**Supplementary Fig. 5i**). Notably, direct IFN-I signals seemed to inhibit *de novo* T_{reg} cell differentiation basally, such that conditioning by bystander inflammation did not further enhance Foxp3 induction in *Ifnar1*^{KO} DR cells.

Together, these data indicate that after bystander inflammation via IFN-I, naive CD4$^+$ T cells are refractory to further proinflammatory signals and are conditioned for enhanced Foxp3$^+$ T_{reg} cell induction. This effect may be due to a partially a cell-intrinsic homeostatic mechanism to limit basal T_{reg} cell induction, perhaps as a mechanism to enable an IFN-I–mediated semi-'primed' state for immune responsiveness[30]. In the wake of inflammatory settings, APCs or stromal cells in the microenvironment that receive IFN-I signals enable an interaction that imparts a state of enhanced receptivity to T_{reg} cell–inducing signals, such that a dynamic state of immune tolerance and increased frequency of T_{reg} cell differentiation is revealed after bystander inflammation.

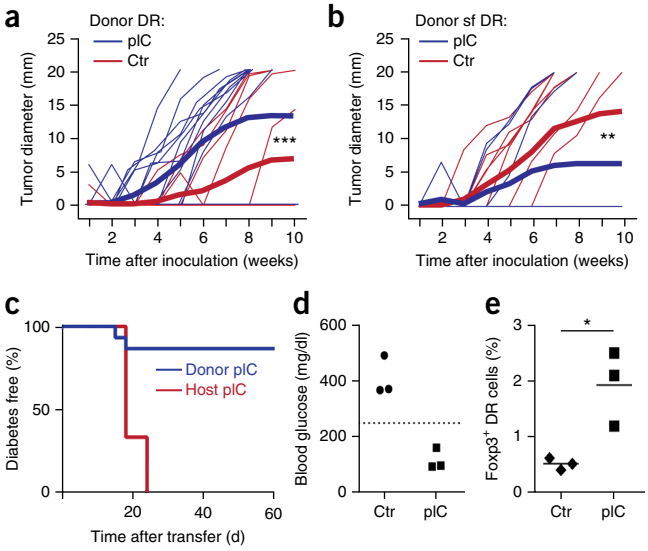

Figure 6 Bystander inflammation conditioning of naive CD4+ T cells inhibits antigen-specific CD4+ T cell responses in a Foxp3-dependent manner. (**a**,**b**) Tumor growth in BALB/c host mice transplanted with CD4+ T cells from control (ctr) or poly(I:C)-treated (pIC) DR mice (**a**) or *Foxp3*-mutant scurfy (sf) DR CD4+ T cells (**b**), immunized with OVA peptide and inoculated subcutaneously 7–10 d later with A20-tGO lymphoma cells. Thin lines represent measurements from individual mice, thick lines represent mean. (**c**) Diabetes-free survival in RIP-mOva–*Rag2*^{KO} host mice that received $_{IC}T_N$ DR cells and were left untreated (donor pIC) or received ctr DR cells and were injected with pIC (host pIC). (**d**,**e**) Blood glucose concentrations (**d**) and frequency of Foxp3+ donor DR cells in pancreatic lymph nodes (**e**) 20 d after pIC treatment of RIP-mOva–*Rag2*^{KO} host mice that received ctr or $_{IC}T_N$ DR CD4 T cells (**Supplementary Fig. 6d**). Each symbol represents a single mouse; horizontal bars represent group mean; representative data from one of two independent experiments, $n = 3$ mice per group. $^*P < 0.05$, $^{**}P < 0.0005$, $^{***}P < 0.0001$, two-way ANOVA (**a**,**b**) or Student's two-tailed *t*-test (**c**). Data are compiled from three independent experiments with $n = 14$ mice per group (**a**) or from two independent experiments, $n = 10$ (**b**,**c**).

$_{IC}T_N$ cell control of antigen-specific response via Foxp3

CD4+ helper T cells have a key role in promoting tumor immunity[31]. However, immunosuppressive mechanisms employed by tumors can support the recruitment and induction of T_{reg} cells that can suppress tumor-specific responses[32,33]. To demonstrate the role of bystander inflammation directly on antigen-specific naive CD4+ T cells in an antitumor response, enriched $_{IC}T_N$ DR cells or control DR cells from PBS-treated mice were transferred into BALB/c hosts, which were then immunized and challenged with OVA-expressing A20 lymphoma cells. BALB/c recipients of $_{IC}T_N$ DR cells showed more robust tumor growth than recipients of control DR cells (**Fig. 6a** and **Supplementary Fig. 6a**), which indicates a direct role for antigen-specific CD4+ T cell suppression of the antitumor response. Notably, this effect was reversed with Foxp3-deficient scurfy DR donors (**Fig. 6b** and **Supplementary Fig. 6b**), which indicates that Foxp3 induction is critical for enhanced tumor tolerance by $_{IC}T_N$ CD4+ T cells.

To better define the role of the antigen-specific naive CD4+ T cell response, we next turned to a model of autoimmune diabetes. In this model, the only T cells present in Rag2-deficient mice expressing membrane-bound OVA under control of a pancreatic islet-specific rat insulin promoter (RIP-mOva × *Rag2*^{KO} host) are donor DR CD4+ T cells, and induction of donor T_{reg} cells is crucial for islet tolerance[8]. Poly(I:C)-mediated bystander inflammation triggered islet autoimmunity and undermined Foxp3 induction in this setting when islet-specific control naive CD4+ T cells encountered antigen[8] (**Fig. 6c**). In contrast, when DR cells were exposed to poly(I:C)-induced inflammation before antigen exposure to generate $_{IC}T_N$ cells, untreated host RIP-mOva–*Rag2*^{KO} mice showed very low incidence of diabetes[8] (**Fig. 6c**). When scurfy DR mice were used as donors, all mice became diabetic regardless of treatment, which underscores the importance of Foxp3 for tolerance in this situation (**Supplementary Fig. 6c**). To test the tolerogenic capacity of $_{IC}T_N$ DR cells, control DR cells from PBS-treated mice or $_{IC}T_N$ DR cells were transferred into RIP-mOva–*Rag2*^{KO} host mice, which were then treated with poly(I:C) (**Supplementary Fig. 6d**). In contrast to recipients of control cells, recipients of $_{IC}T_N$ DR cells had normal blood glucose concentrations at day 20 after transfer (**Fig. 6d**). Furthermore, Foxp3+ T_{reg} cell frequencies were higher among the $_{IC}T_N$ donor DR cells than controls, which demonstrates that this process of enhanced T_{reg} cell induction after bystander inflammation can occur even in conditions that are highly unfavorable to Foxp3 induction (**Fig. 6e**).

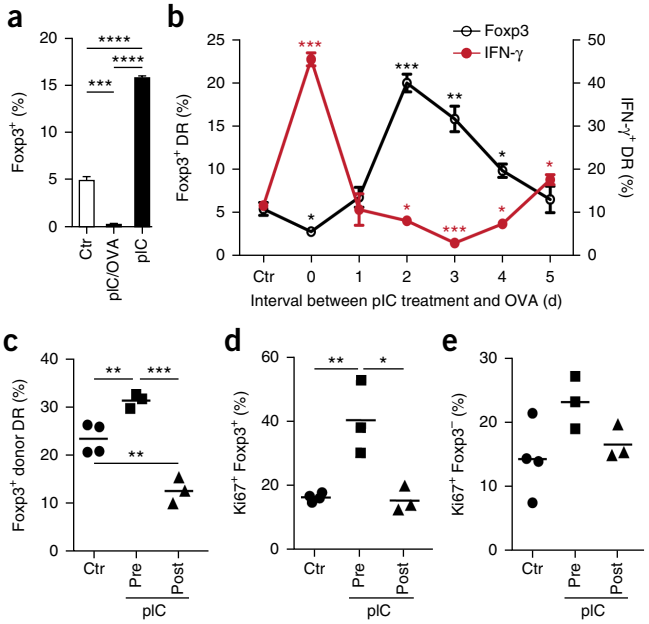

Figure 7 Timing of bystander inflammation relative to antigen signal determines conditioning for regulatory versus effector cell differentiation. (**a**) Percentage of Foxp3+ DR cells from CD4+ T cells isolated from DR mice treated with PBS (ctr), poly(I:C) alone (pIC) or poly(I:C) and OVA peptide (pIC/OVA) on two consecutive days, and cultured with OVA-pulsed APC and TGF-β for 3 d. (**b**) Percentage of IFN-γ+ and Foxp3+ DR cells in spleen and lymph node cells harvested at different time points after treatment with pIC from DR-cell recipients, cultured with OVA-pulsed APCs and TGF-β for 5 d and stimulated with PMA and ionomycin (**Supplementary Fig. 7a**). (**c**–**e**) Percentage of Foxp3+ (**c**), Ki67+Foxp3+ (**d**) and Ki67+Foxp3− (**e**) donor DR cells from mesenteric lymph node (LN) of BALB/c host mice that were treated with PBS (ctr) or pIC 2–3 d before (pre) or 1–2 d after (post) addition of OVA protein in drinking water (Online Methods). Each symbol represents an individual mouse; horizontal bars represent group mean; data are representative of two independent experiments, $n \geq 6$ mice per group. Data are mean ± s.e.m. of three replicates (**a**,**b**) or representative of two independent experiments, $n = 2$ mice per group. $^*P < 0.05$, $^{**}P < 0.001$, $^{***}P < 0.0001$, $^{****}P < 0.00001$, Student's two-tailed *t*-test (**a**–**d**).

Timing of inflammation controls $_{IC}T_N$ response

Our findings suggest that the timing of bystander inflammation relative to antigen encounter is involved in the determination of T_{reg} and T_{eff} cell differentiation. Indeed, comparison of cultured DR cells from mice treated with poly(I:C) alone or poly(I:C) plus OVA peptide showed that T_{reg} cell induction was diminished by concurrent signals and enhanced by decoupling of signals (**Fig. 7a**). To investigate the temporal role of bystander inflammation relative to antigen encounter, we transferred DR cells into BALB/c host mice, which were then administered injections of poly(I:C) at one of six time points (from 5 d before to day of lymphocyte harvest). Lymphocytes were then harvested and cultured with OVA-pulsed APCs in the presence of TGF-β (**Supplementary Fig. 7a**). Expression of PD-L1, CD69 and Ly6C—surface molecules associated with antigen-independent bystander inflammation—was transient in donor DR cells (**Supplementary Fig. 7b**). Donor DR cell frequencies were consistent among all time points, which indicates that these cells are not subject to substantial attrition after bystander inflammation (**Supplementary Fig. 7c**). Notably, assessment of intracellular Foxp3 and IFN-γ abundance indicated that T_{eff} cell differentiation was markedly enhanced when bystander inflammation and antigen encounter were temporally coordinated (time point 0), whereas T_{reg} cell induction was enhanced when inflammation and antigen encounter were separated by 2–3 d; expression of both markers returned to levels similar to that in PBS-treated controls at the latest time points (**Fig. 7b**). This effect was confirmed *in vivo* using antigen-specific T_{reg} cell induction by oral antigen delivery (**Fig. 7c**). Furthermore, proliferation of induced T_{reg} cells, but not Foxp3$^-$ cells, was enhanced by exposure to bystander inflammation before antigen; this further supports a role for pre-exposure to inflammation in the increased numbers of induced Foxp3$^+$ T_{reg} cells upon cognate antigen recognition (**Fig. 7d**,**e**). Together, these data show that nonspecific bystander inflammation can condition naive CD4$^+$ T cells to 'favor' T_{eff} cell or T_{reg} cell differentiation under different circumstances, and this conditioning is linked to the relative timing of antigen and inflammatory signals.

DISCUSSION

In this study we sought to determine how nonspecific bystander inflammation in the absence of cognate antigen stimuli affects CD4$^+$ T cell responses. Our results show that the process of bystander inflammation can inhibit the immune response to antigen by conditioning of naive CD4$^+$ T cells to be refractory to T_{eff} cell differentiation and to enhance T_{reg} cell induction. We showed that the effect of such bystander conditioning can be modulated by the temporal relationship of the inflammation and antigen signals such that coordinated signals undermine T_{reg} cell induction and temporally decoupled signals enhance T_{reg} cell induction. These results suggest a paradigm for T cell priming signals and reveal an underlying principle for the apparent duality of the role of innate inflammation as both a driver and inhibitor of T cell responses[12,13].

The effects of bystander inflammation on subsequent T cell differentiation were greatest at suboptimal differentiation conditions. This characteristic would be consistent with the idea that the refractory state of naive T cells after bystander inflammation acts as a temporary buffer to prevent unwanted autoimmune responses while still preserving the ability to adjust immune responses according to need. Notably, impaired antitumor immunity in the presence of $_{IC}T_N$ DR cells was reversed when these cells did not express functional Foxp3. This would suggest that Foxp3 itself has an important role as a component of a 'master switch' molecular complex that guides T_{reg} cell differentiation in $_{IC}T_N$ CD4$^+$ T cells. Furthermore, our findings supports the idea that pro-effector molecular factors are also mobilized in this process and that the end result of T cell differentiation depends on the balance of these factors[34]. Although our results do not directly demonstrate a Foxp3-dependent control switch for T_{eff} versus T_{reg} cell induction in this context, lineage-tracing approaches support the idea that transient low-level *de novo* Foxp3 expression occurs in CD4$^+$ T cells in inflammatory contexts[35].

Bystander inflammation conditioning of naive CD4$^+$ T cells was dependent on IFN-I, a critical component of TLR-mediated optimization of T cell responses[36]. Our adoptive transfer experiments suggest that IFN-I signals can have a direct role on antigen-specific CD4$^+$ T cells as well as other cells in the microenvironment to mediate anti- and pro-induction effects on Foxp3. Although not as apparent in monoclonal DR *Ifnar1*^{KO} mice, this effect was revealed in the context of the lymphoreplete environment, which suggests a role for other lymphocyte subsets (such as B cells and T_{reg} cells) for this effect. Upon enhanced IFN-I signal during poly(I:C)-mediated bystander inflammation, IFN-I signal action on the surrounding cells in the microenvironment mediated a release of this basal inhibition of Foxp3, resulting in an apparent increase in frequency of *de novo* T_{reg} cell induction among wild-type DR cells. IFN-I has a complex role as an immunomodulatory cytokine, both as a promoter and inhibitor of antigen-specific immune responses[37]. In the Clone 13 model of chronic LCMV infection, IFN-I receptor blockade can initiate CD4$^+$ T cell–dependent viral clearance[38,39]. Additionally, the immunosuppressive role of IFN-I in chronic LCMV has been linked to suppression of mechanisms of type I T_{eff} cell differentiation[40,41]. These studies have demonstrated a clearly reversible refractory state. Similarly, we have shown that the same bystander inflammatory response can undermine or enhance T_{reg} cell induction, depending on its temporal relationship with antigen encounter. These lines of evidence suggest the possibility that quiescent naive CD4$^+$ T cells adjust the qualitative nature of their response to antigen in a dynamic manner that corresponds to temporal windows defined by environmental cues.

The physiological impact of the differentiation outcomes for $_{IC}T_N$ CD4$^+$ T cells has notable ramifications for health and disease. The results presented here highlight a dimension of CD4$^+$ T cell biology, namely the ability of naive T cells to modulate response to antigen by integration of signals over time. This type of molecular coordination probably evolved to mitigate potential for autoimmunity after cellular damage and release of self-antigens during infection. Indeed, epidemiological data support the notion that environmental conditioning of the immune system by infection diminishes the aberrant immune responses that lead to autoimmunity[42]. The flip side of this immunoregulatory process is enhanced susceptibility to heterologous superinfection and immune escape of tumors. As the antiparallel to autoimmunity, tumor immunity is similarly complicated by conflicting roles for the immunomodulatory role of inflammatory responses[43,44]. The interplay of inflammatory processes acting *in trans* on the homeostatic immune and tissue-supporting microenvironment may even have an important role in early progression of tumorigenesis[45,46]. It is conceivable that the process of tumorigenesis in the context of infectious or tumor-derived inflammation could be enhanced by conditioning of newly infiltrating naive T cells for *de novo* T_{reg} cell induction during the process of immunoediting. Such an effect could partially account for the relentless growth and metastasis of tumors despite relatively high levels of immune cell infiltration compared to healthy tissues.

Crucial for an effective but nonharmful immune response by T cells is the integration of positive and negative feedback signaling over time. By providing signals to alter the quality of responses

during the course of a response to infection, we propose that the inflammatory milieu produced by innate immune mechanisms coordinates effector and regulatory lymphocyte responses as a series of waves that promote both immunity and self-tolerance. As an evolutionary adaptation, this process is probably a component of the 'metastable equilibrium' that enables sustainable levels of viral control without deleterious immunopathology during intractable chronic infection[47]. These concepts may be useful for lending nuance to vaccine and immunotherapeutic approaches to achieve more finely tuned outcomes.

METHODS

Methods and any associated references are available in the online version of the paper.

Note: Any Supplementary Information and Source Data files are available in the online version of the paper.

ACKNOWLEDGMENTS

We thank D. Campbell, J. Hamerman and E. Bettelli for helpful discussion, and S. Ma and Aru K. for technical assistance. We thank A. Abbas, M. Orr and A. Marshak-Rothstein for mice and materials. Supported by American Cancer Society postdoctoral fellowship 121930-PF-12-071-01-LIB and National Institute of Allergy and Infectious Diseases (NIAID) grant T32 AI007411 (L.J.T.) and the Juvenile Diabetes Research Foundation Cooperative Center for Cellular Therapy and US National Institutes of Health grant CA182783 (S.F.Z.).

AUTHOR CONTRIBUTIONS

L.J.T. and S.F.Z. developed the study. L.J.T. and J.-F.L. designed and performed the experiments. A.C.V., T.D.T. and Z.L.U. performed *in vitro* experiments. L.J.T. and S.F.Z. wrote the manuscript, and all authors contributed to manuscript editing.

COMPETING FINANCIAL INTERESTS

The authors declare no competing financial interests.

1. Yoshimura, A., Naka, T. & Kubo, M. SOCS proteins, cytokine signalling and immune regulation. *Nat. Rev. Immunol.* **7**, 454–465 (2007).
2. Schmitz, M.L., Weber, A., Roxlau, T., Gaestel, M. & Kracht, M. Signal integration, crosstalk mechanisms and networks in the function of inflammatory cytokines. *Biochim. Biophys. Acta* **1813**, 2165–2175 (2011).
3. Scott-Browne, J.P. *et al.* Expansion and function of Foxp3-expressing T regulatory cells during tuberculosis. *J. Exp. Med.* **204**, 2159–2169 (2007).
4. Haribhai, D. *et al.* A requisite role for induced regulatory T cells in tolerance based on expanding antigen receptor diversity. *Immunity* **35**, 109–122 (2011).
5. Bilate, A.M. & Lafaille, J.J. Induced CD4$^+$Foxp3$^+$ regulatory T cells in immune tolerance. *Annu. Rev. Immunol.* **30**, 733–758 (2012).
6. Janeway, C.A. Jr. & Medzhitov, R. Innate immune recognition. *Annu. Rev. Immunol.* **20**, 197–216 (2002).
7. van Duin, D., Medzhitov, R. & Shaw, A.C. Triggering TLR signaling in vaccination. *Trends Immunol.* **27**, 49–55 (2006).
8. Thompson, L.J., Valladao, A.C. & Ziegler, S.F. Cutting edge: *de novo* induction of functional Foxp3$^+$ regulatory CD4 T cells in response to tissue-restricted self antigen. *J. Immunol.* **186**, 4551–4555 (2011).
9. Srivastava, S., Koch, M.A., Pepper, M. & Campbell, D.J. Type I interferons directly inhibit regulatory T cells to allow optimal antiviral T cell responses during acute LCMV infection. *J. Exp. Med.* **211**, 961–974 (2014).
10. Coffman, R.L., Sher, A. & Seder, R.A. Vaccine adjuvants: putting innate immunity to work. *Immunity* **33**, 492–503 (2010).
11. Boyman, O. Bystander activation of CD4$^+$ T cells. *Eur. J. Immunol.* **40**, 936–939 (2010).
12. Christen, U. & von Herrath, M.G. Do viral infections protect from or enhance type 1 diabetes and how can we tell the difference? *Cell. Mol. Immunol.* **8**, 193–198 (2011).
13. Mills, K.H. TLR-dependent T cell activation in autoimmunity. *Nat. Rev. Immunol.* **11**, 807–822 (2011).
14. Bach, J.F. Infections and autoimmune diseases. *J. Autoimmun.* **25** (suppl.) 74–80 (2005).
15. Headley, M.B. *et al.* TSLP conditions the lung immune environment for the generation of pathogenic innate and antigen-specific adaptive immune responses. *J. Immunol.* **182**, 1641–1647 (2009).
16. Durrant, D.M. & Metzger, D.W. Emerging roles of T helper subsets in the pathogenesis of asthma. *Immunol. Invest.* **39**, 526–549 (2010).
17. Saff, R.R., Spanjaard, E.S., Hohlbaum, A.M. & Marshak-Rothstein, A. Activation-induced cell death limits effector function of CD4 tumor-specific T cells. *J. Immunol.* **172**, 6598–6606 (2004).
18. Takahashi, R. *et al.* SOCS1 is essential for regulatory T cell functions by preventing loss of Foxp3 expression as well as IFN-γ and IL-17A production. *J. Exp. Med.* **208**, 2055–2067 (2011).
19. Lu, L.F. *et al.* Foxp3-dependent microRNA155 confers competitive fitness to regulatory T cells by targeting SOCS1 protein. *Immunity* **30**, 80–91 (2009).
20. Haxhinasto, S., Mathis, D. & Benoist, C. The AKT-mTOR axis regulates *de novo* differentiation of CD4$^+$Foxp3$^+$ cells. *J. Exp. Med.* **205**, 565–574 (2008).
21. Delgoffe, G.M. *et al.* The mTOR kinase differentially regulates effector and regulatory T cell lineage commitment. *Immunity* **30**, 832–844 (2009).
22. Yamane, H. & Paul, W.E. Early signaling events that underlie fate decisions of naive CD4$^+$ T cells toward distinct T-helper cell subsets. *Immunol. Rev.* **252**, 12–23 (2013).
23. Wei, J. *et al.* Antagonistic nature of T helper 1/2 developmental programs in opposing peripheral induction of Foxp3$^+$ regulatory T cells. *Proc. Natl. Acad. Sci. USA* **104**, 18169–18174 (2007).
24. Bettelli, E. *et al.* Reciprocal developmental pathways for the generation of pathogenic effector TH17 and regulatory T cells. *Nature* **441**, 235–238 (2006).
25. Wang, Y. *et al.* Timing and magnitude of type I interferon responses by distinct sensors impact CD8 T cell exhaustion and chronic viral infection. *Cell Host Microbe* **11**, 631–642 (2012).
26. Barchet, W. *et al.* Virus-induced interferon-α production by a dendritic cell subset in the absence of feedback signaling *in vivo*. *J. Exp. Med.* **195**, 507–516 (2002).
27. Matsumoto, M. & Seya, T. TLR3: interferon induction by double-stranded RNA including poly(I:C). *Adv. Drug Deliv. Rev.* **60**, 805–812 (2008).
28. Liu, Y. *et al.* FoxA1 directs the lineage and immunosuppressive properties of a novel regulatory T cell population in EAE and MS. *Nat. Med.* **20**, 272–282 (2014).
29. Dumont, F.J. & Coker, L.Z. Interferon-α/β enhances the expression of Ly-6 antigens on T cells *in vivo* and *in vitro*. *Eur. J. Immunol.* **16**, 735–740 (1986).
30. Taniguchi, T. & Takaoka, A. A weak signal for strong responses: interferon-α/β revisited. *Nat. Rev. Mol. Cell Biol.* **2**, 378–386 (2001).
31. Knutson, K.L. & Disis, M.L. Tumor antigen-specific T helper cells in cancer immunity and immunotherapy. *Cancer Immunol. Immunother.* **54**, 721–728 (2005).
32. Zhou, G., Drake, C.G. & Levitsky, H.I. Amplification of tumor-specific regulatory T cells following therapeutic cancer vaccines. *Blood* **107**, 628–636 (2006).
33. Zhou, G. & Levitsky, H.I. Natural regulatory T cells and *de novo*-induced regulatory T cells contribute independently to tumor-specific tolerance. *J. Immunol.* **178**, 2155–2162 (2007).
34. Zhou, L. *et al.* TGF-β-induced Foxp3 inhibits T_H17 cell differentiation by antagonizing RORγt function. *Nature* **453**, 236–240 (2008).
35. Miyao, T. *et al.* Plasticity of Foxp3$^+$ T cells reflects promiscuous Foxp3 expression in conventional T cells but not reprogramming of regulatory T cells. *Immunity* **36**, 262–275 (2012).
36. Longhi, M.P. *et al.* Dendritic cells require a systemic type I interferon response to mature and induce CD4$^+$ Th1 immunity with poly IC as adjuvant. *J. Exp. Med.* **206**, 1589–1602 (2009).
37. González-Navajas, J.M., Lee, J., David, M. & Raz, E. Immunomodulatory functions of type I interferons. *Nat. Rev. Immunol.* **12**, 125–135 (2012).
38. Teijaro, J.R. *et al.* Persistent LCMV infection is controlled by blockade of type I interferon signaling. *Science* **340**, 207–211 (2013).
39. Wilson, E.B. *et al.* Blockade of chronic type I interferon signaling to control persistent LCMV infection. *Science* **340**, 202–207 (2013).
40. Stelekati, E. *et al.* Bystander chronic infection negatively impacts development of CD8$^+$ T cell memory. *Immunity* **40**, 801–813 (2014).
41. Osokine, I. *et al.* Type I interferon suppresses *de novo* virus-specific CD4 Th1 immunity during an established persistent viral infection. *Proc. Natl. Acad. Sci. USA* **111**, 7409–7414 (2014).
42. Bach, J.F. The effect of infections on susceptibility to autoimmune and allergic diseases. *N. Engl. J. Med.* **347**, 911–920 (2002).
43. Dunn, G.P., Koebel, C.M. & Schreiber, R.D. Interferons, immunity and cancer immunoediting. *Nat. Rev. Immunol.* **6**, 836–848 (2006).
44. Grivennikov, S.I., Greten, F.R. & Karin, M. Immunity, inflammation, and cancer. *Cell* **140**, 883–899 (2010).
45. Trinchieri, G. Cancer and inflammation: an old intuition with rapidly evolving new concepts. *Annu. Rev. Immunol.* **30**, 677–706 (2012).
46. Conroy, H., Marshall, N.A. & Mills, K.H. TLR ligand suppression or enhancement of Treg cells? A double-edged sword in immunity to tumours. *Oncogene* **27**, 168–180 (2008).
47. Virgin, H.W., Wherry, E.J. & Ahmed, R. Redefining chronic viral infection. *Cell* **138**, 30–50 (2009).

ONLINE METHODS

Mice. BALB/cAnNCrl (BALB/c) and C57BL/6NCrl (B6) mice were purchased from Charles River Laboratories. C.B6(Cg)-Rag2$^{tm1.1Cgn}$/J (*Rag2*^{KO}), C.Cg-Tg(DO11.10)10Dlo/J (DO11.10) and B.Cg-Foxp3^{sf}/J (scurfy) mice were purchased from Jackson Laboratories. Scurfy mice were backcrossed >11 generations to BALB/c background. Transgenic mice expressing membrane-bound OVA under control of the rat insulin promoter (RIP-mOVA) mice on BALB/c background were provided by A. Abbas (UCSF). *Ifnar1*^{KO} mice on BALB/c background were provided by M. Orr (Infectious Disease Research Institute). Sex-matched male and female mice aged 8–12 weeks were used. No specific exclusion criteria were used in mouse experiments. Animals were housed in Specific Pathogen Free facilities and experiments were conducted in accordance with the Animal Care and Use Committee at the Benaroya Research Institute.

Tumor studies. A20-tGO lymphoma cells expressing OVA were a gift from A. Marshak-Rothstein (University of Massachusetts). Tumor cells were tested for murine pathogens, including *Mycoplasma* spp., before use (IMPACT pathogen test, IDEXX BioResearch). *In vivo* tumor studies using A20-tGO cells were conducted as described[17]. Briefly, tumor cells were expanded *in vitro* in complete RPMI with G418 (Invitrogen). Mice were inoculated subcutaneously with 1×10^6 live tumor cells in the flank. Tumor growth was assessed by direct measurement of the maximum diameter of palpable tumor mass. Mice with tumor diameter >15 mm were considered at experimental endpoint.

***In vivo* induction of bystander activation and immunizations.** High molecular-weight poly(I:C) was purchased from Invivogen. For systemic *in vivo* responses, 100 µg of poly(I:C) was injected intraperitoneally for 2 consecutive days. Where indicated, 50 µg of OVA 323–339 peptide (Anaspec) was injected intraperitoneally (i.p.) with poly(I:C) 14–18 h after the last injection, and spleen and peripheral lymph nodes were harvested for cell preparations. For intranasal delivery of poly(I:C), mice were anesthetized with isoflurane, and 25 µg poly(I:C) was aspirated into the nostril via pipette. Immunization with whole OVA protein (Sigma) was via subcutaneous injection in IFA (Sigma) emulsion. To assess DR response to oral OVA treatment, DR cells were parked in BALB/c host mice, which then received OVA-supplemented drinking water (1% w/v) for 3–4 d, and mesenteric lymph node (LN) cells were analyzed 7 d after start of OVA feeding. LCMV-Armstrong was provided by D. Campbell (Benaroya Research Institute). Mice were inoculated with 2×10^5 plaque-forming units (p.f.u.) LCMV via i.p. injection.

Induction of asthma. Recombinant murine thymic stromal lymphopoietin (TSLP) was a gift from Amgen. For short-term acute asthma induction (**Supplementary Fig. 1g**), mice were primed intranasally with OVA and TSLP using a modification of the protocol described[15]. Briefly, mice were treated with 50 µg poly(I:C) or PBS intranasally on days −2 and −1, primed with OVA (25 µg) and TSLP (20 µg) on days 0 and 3 then challenged with intranasal OVA (25 µg) for 2 consecutive days starting on day 7–9. Two to three days after the first OVA challenge, mice were euthanized, and single-cell suspensions of perfused lung tissue were assessed by flow cytometry. For airway inflammation memory T cell response (**Supplementary Fig. 2a**), mice were treated with 100 µg poly(I:C) or PBS i.p. on days −3 and −2 then immunized subcutaneously with OVA (50 µg) emulsified in IFA on day 0, and 12–14 d later were challenged with one dose of OVA with TSLP as described above, followed by two consecutive doses of OVA only. Two days after the last challenge dose, mice were euthanized, and perfused lung tissue was assessed. A minimum of 6 mice per group ($n \geq 3$ per experiment) was used to achieve reasonable statistical power.

Mouse diabetes model. *Rag2*^{KO} DO11.10 mice (DR mice) with transgenic T cell receptor recognizing OVA epitope 232–339 in the context of I-A^d class II major histocompatibility complex were used for donor T cells. Purified CD4$^+$ T cells from DR donor mice were transferred into RIP-mOVA–*Rag2*^{KO} host mice. Donor or host mice were treated as described in figure legends (**Fig. 6c–e** and **Supplementary Fig. 6c,d**). Mice were evaluated for diabetes by blood glucose monitoring using Ascencia Contour glucometer system (Bayer AG). Mice were considered diabetic upon 2 consecutive daily blood glucose measurements exceeding 250 mg/dl.

Flow cytometry and sorting. Antibodies for cell surface staining for CD4 (RM4-5), D011.10 TCR (KJ1-26), CD25 (eBio3C7), CD44 (IM7), CD62L (MEL-14), GITR (YGITR 765), Ly6G (1A8), Ly6C (HK1.4), CD45.1 (A20), CD45.2 (104), B220 (RA3-6B2), MHC class II (M5/114.15.2), CD11b (M1/70), CD3 (2C11), Siglec-F (E50-2440) and CD11c (N418) were purchased from eBioscience, Biolegend or BD Biosciences. Unlabeled anti-CD3 (145-2C11) and anti-CD28 (PV-1) were purchased from the University of California San Francisco Antibody Core. Intracellular staining for Foxp3 (FJK-16s), T-bet (4B10), IFN-γ (XMG1.2), IL-17A (TC11-18H10.1), IL-10 (JES5-16E3), K_i-67 (B56) (eBioscience, Biolegend or BD Biosciences) was conducted using eBioscience Foxp3 intracellular staining reagents according to the manufacturer's instructions. Intracellular staining for phospho-STAT1 (4a) (BD Biosciences), phospho-SMAD2/3 (D27F4), p-AKT (D9E) and p-S6 ribosomal protein (D57.2.2E) (Cell Signaling Technology) was conducted as described[48]. Antibody validation profiles were verified via CiteAb (http://www.citeab.com). Naive CD4$^+$ T cells were isolated using no-touch magnetic bead purification (MACS, Miltenyi Biotec). Where indicated, cells were further sorted as described by florescent antibody labeling using FACSAria cell sorting system (BD Biosciences). Flow cytometric analysis used LSRII, Canto, and FACSCalibur cytometers (BD Biosciences), and data were analyzed with FlowJo Software.

***In vitro* cultures.** For *in vitro* bystander activation, 3 µg/ml poly(I:C) or 100 U/ml recombinant IFN-β (R&D Systems) was used. To block IFN-I signaling, 10 µg/ml anti-IFNAR1 (MAR1-5A3, eBioscience) was used. To test *in vitro* T_{reg} cell suppression, sorted CD25$^+$CD4$^+$ T cells were mixed with CFSE-labeled naive CD62L^{hi}CD44^{lo}CD25$^-$CD4$^+$ T cells at different ratios. Naive T cells with no T_{reg} cells were used as controls. Sorted cells were mixed with irradiated *Rag2*^{KO} splenocytes and stimulated with 0.1 µg/ml plate-bound anti-CD3 and assessed by flow cytometry 2 d later. CFSE dilution of non-T_{reg} CD4$^+$ T cells was used to calculate proliferation index of responding cells[49], and activation of responding non-T_{reg} CD4$^+$ T cells was assessed by surface CD25 and intracellular T-bet. For *in vitro* T cell cultures, spleen and lymph nodes were processed to single-cell suspensions, and naive CD4$^+$ T cells were isolated as described above. T cells were then mixed at a 1:3 or 1:4 ratio with irradiated splenocytes from naive *Rag2*^{KO} donors, and T cell receptor stimulation was achieved as indicated by either addition of OVA 323–339 peptide or plate-bound anti-CD3 (UCSF Antibody Core). Various concentrations of recombinant human TGF-β (Peprotech) were added to cultures as indicated, and cells were analyzed by flow cytometry 3–5 d later. Except as specified in figure legends, 1–2 ng/ml TGF-β was used. For *in vitro* cultures, data are shown as mean and s.e.m. of three technical replicates for each condition, representing a single mouse. *n* designates independent experiments or mice. For intracellular cytokine analysis, day 5 cultures were restimulated with either plate-bound anti-CD3 and anti-CD28 (5 µg/ml and 1 µg/ml, respectively) or PMA and ionomycin in the presence of Golgi inhibitor (BD Pharmingen) for 5 h. Blocking antibodies anti-PDL1 (clone 10F.9G2, eBioscience), anti-IL10 (clone JES5-2A5, UCSF Antibody Core), and isotype control (rat IgG2a) were used at final concentration of 10 µg/ml in culture. 1-MT (Sigma) was reconstituted in NaOH and pH adjusted to 7 to make a stock concentration of 20 mM, and added to culture medium at a final concentration of 100 µM[50]. Cultured cells were stained with live/dead cell stain (Fixable Viability Dye, eBioscience) before antibody staining. Cells were cultured in complete RPMI (Sigma) with 5% FBS (Sigma).

Analysis of gene expression. Cell pellets containing equivalent cell numbers were resuspended in Qiazol lysis buffer and RNA was isolated using miRNeasy total RNA isolation kit (Qiagen). Protocols for mRNA or miRNA sample preparation were according to the manufacturer's instructions. cDNA was generated with Primescript Reverse Transcriptase (Clontech) or Multiscribe reverse transcriptase (Life Technologies). TaqMan probes (Life Technologies) were used for *Socs1*, *Socs3*, *Mir155*, *Il12rb2* and *Tbx21*, with *Rn18s* and *Sno234* for normalization controls for mRNA and miRNA, respectively. Other quantitative

doi:10.1038/ni.3329

PCR (qPCR) primer sequences for use with SYBR Green reagents (Sigma) were as follows: *Ifnar1* F 5′-AGCCACGGAGAGTCAATGG-3′; *Ifnar1* R 5′-GCTCTGACACGAAACTGTGTTTT-3′; *Ifnar2* F CTTCGTGTTTGGTAGTGATGGT-3′; *Ifnar2* R 5′-GGGGATGATTTCCAGCCGA-3′; *Tgfbr1* F 5′-TCCAAACAGATGGCAGAGC-3′; *Tgfbr1* R 5′-TCCATTGGCATACCAGCAT-3′. For normalization controls, primers for *Gapdh* F 5′-TCCATGACAACTTTGGCATTG-3′ and *Gapdh* R 5′-CAGTCTTCTGGGTGGCAGTGA-3′ were used. Samples were acquired on ABI 7500 RT-PCR system.

***Foxp3* promoter methylation analysis.** Cells were harvested as indicated in figure legends (**Supplementary Fig. 4b**), and DNA isolation and bisulfite conversion using Epitect Plus DNA bisulfite conversion kit (Qiagen) according to the manufacturer's instructions. Analysis of *Foxp3* promoter sequence conversion was conducted as described[51]. Samples were obtained from 3 mice per group, and 8–10 sequences per sample were analyzed.

Statistics. Statistical analysis tests were calculated with Prism 5 (GraphPad) analysis software. Statistical tests used and estimates of variation within groups were based on published results using similar approaches. Assumption of equal variance was applied to all statistical tests except where stated in figure legends. No randomization was done for animal studies, and investigators were not blinded to experimental group allocations.

48. Koch, M.A. *et al.* T-bet^{+} Treg cells undergo abortive Th1 cell differentiation due to impaired expression of IL-12 receptor-β2. *Immunity* **37**, 501–510 (2012).
49. Lyons, A.B. Analysing cell division *in vivo* and *in vitro* using flow cytometric measurement of CFSE dye dilution. *J. Immunol. Methods* **243**, 147–154 (2000).
50. Mellor, A.L. *et al.* Cutting edge: CpG oligonucleotides induce splenic CD19^{+} dendritic cells to acquire potent indoleamine 2,3-dioxygenase-dependent T cell regulatory functions via IFN Type 1 signaling. *J. Immunol.* **175**, 5601–5605 (2005).
51. Floess, S. *et al.* Epigenetic control of the foxp3 locus in regulatory T cells. *PLoS Biol.* **5**, e38 (2007).